

Human-Inspired Control Logic for Automated Maneuvering of Miniature Helicopter

V. Gavrilets,* B. Mettler,[†] and E. Feron[‡]

Massachusetts Institute of Technology, Cambridge, Massachusetts 02139

The maneuvering control logic that was developed to implement aerobatic maneuvers fully automatically on a miniature helicopter is described. The key component of this system is a state-machine maneuver execution logic that was inspired by an analysis of human pilot strategies. Conventional multivariable trim trajectory controllers were used before and on the exit from the maneuvers; bumpless transfer between these control modes was achieved through re-initialization of controller integrator states. Flight tests with this control logic demonstrated smooth maneuver entry, automatic recovery to a steady-state trim trajectory, and an ability to sequence maneuvers in a fully autonomous airshow-like sequence. This approach was flight tested with split-S, hammerhead, and 360-deg axial roll maneuvers, as well as a split-S-hammerhead maneuver sequence. The maneuvering control logic can be used to automate a variety of other maneuvers.

Introduction

UNMANNED aerial vehicles increasingly play critical roles in military surveillance and reconnaissance applications. These vehicles, which mainly consist of fixed-wing aircraft, are flown well above ground to prevent detection and avoid exposure to threats. Future roles will include operations such as weapon delivery, air and ground combat, as well as accurate sensor placement, payload delivery, and retrieval.¹ Such applications will expose the vehicles to a range of threats as well as complex environments. Similar to manned operations,² a key success factor for such applications will be the ability to maneuver the aircraft with agility. Miniature rotorcraft, such as those used by hobby remote-control (R/C) pilots, have already demonstrated unparalleled maneuvering abilities and, therefore, could be good candidates for applications requiring highly agile flight, such as for urban surveillance and warfare. These miniature vehicles are being used in a few commercial applications, mainly in the filming industry where they are used to produce dynamic birds-eye footage.

Miniature helicopters are capable of a wide range of extreme maneuvers. The unique maneuvering capabilities of these vehicles are due to a combination of special design, for example, stiff rotor heads, and physical scaling effects. Small-scale vehicles (of about 1/10th rotor diameter) designed for aerobatic flight enjoy disproportionately large control forces and moments.³ They are typically characterized by thrust-to-weight ratios that exceed two, and peak roll- and pitch-rate sensitivities of about 200 deg/s. The latter are limited artificially by a stabilizer bar⁴ to help the human pilot. Many R/C helicopters can also produce a negative rotor thrust, large enough to sustain inverted flight.

In contrast, due to physical constraints, most full-scale helicopters have small thrust margins (10–20%) (Ref. 5) and are not designed to sustain extreme attitude angles nor high g loadings, which limits

their maneuvering capabilities. Small-scale helicopters can perform maneuvers that are impossible for full-scale helicopters. Extreme maneuvering with full-scale vehicles sets extreme requirements on the powerplant, rotor, and other structural elements. More recent combat helicopters featuring hingeless rotors, for example, Boeing's Apache or Eurocopter's Tiger helicopters, have demonstrated basic aerobatic capabilities, performing rolls and loops.

Many modern control applications to full-scale rotorcraft involve partial authority systems. These are aimed at improving handling qualities and effectively addressing the resulting design tradeoffs.^{6,7} Because full-scale vehicles are subject to more stringent physical limitations, active control technologies have also been developed to cue the pilot when approaching limitations⁸; these systems should help the pilot better exploit the inherent aircraft performance and attain higher levels of agility. Higher authority systems have also been proposed. One of the first helicopter autopilots was developed in the late 1960s–early 1970s for a CH-53A helicopter.² The autopilot, developed with classical control techniques, was capable of waypoint navigation and automatic nap-of-the-earth terrain following. More recently, Osder and Caldwell⁹ have proposed a procedure for the design of a full-envelope fly-by-wire control system. The system has been validated on an AH-64 Apache helicopter.

Previous experimental work on automatic control of miniature helicopters concentrated on tracking trim trajectories. La Civita et al.¹⁰ have successfully flight tested an H-infinity loop shaping controller on a Yamaha R-50 helicopter. Kannan and Johnson¹¹ have implemented a neural-network-based adaptive controller on the newer Yamaha RMAX helicopter. In both cases, accurate tracking of simple trajectories at moderate speeds was achieved. The Yamaha helicopters are one order of magnitude heavier than the X-Cell and have dynamic characteristics that are closer to conventional full-scale helicopters³ and, thus, are not capable of extreme maneuvering.

Because of the fast and large responses to control inputs and the lack of inherent stability of the aircraft, flying small-scale R/C helicopters requires a very skilled pilot; only a few can exploit the range of maneuvering capabilities of these aircraft. Figure 1 shows a split-S, a maneuver that involves a half-roll, inverted flight, followed by a half-loop, which finally ends at level flight in the reversed flight direction. Linear feedback controllers, like those used in typical aviation autopilots^{12,13} or those used in miniature rotorcraft, are not suited for extreme maneuvering due to the highly nonlinear dynamic behavior encountered when maneuvers such as split-S are executed.

Frazzoli¹⁴ suggested a nonlinear control design method for helicopters based on a so-called backstepping approach. The central idea in his approach is to determine desired main rotor thrust and orientation based on translational commands (velocity or position) and then use the control moments to orient the rotor in the desired direction. The tail rotor thrust is used primarily to counteract the

Received 1 January 2003; accepted for publication 20 January 2004. Copyright © 2004 by the authors. Published by the American Institute of Aeronautics and Astronautics, Inc., with permission. Copies of this paper may be made for personal or internal use, on condition that the copier pay the \$10.00 per-copy fee to the Copyright Clearance Center, Inc., 222 Rosewood Drive, Danvers, MA 01923; include the code 0731-5090/04 \$10.00 in correspondence with the CCC.

*Research Assistant, Laboratory for Information and Decision Systems, Department of Aeronautics and Astronautics; currently Manager of Control Systems Development, Athena Technologies, Manassas, VA 20110; vgavrilets@athenati.com.

[†]Postdoctoral Associate, Laboratory for Information and Decision Systems, Department of Aeronautics and Astronautics; bmettler@mit.edu. Associate Member AIAA.

[‡]Associate Professor of Aeronautics and Astronautics, Laboratory for Information and Decision Systems; feron@mit.edu. Senior Member AIAA.



Fig. 1 Split-S maneuver, which consists of a half-roll followed by a half-loop; result is a reversal of the flight direction (picture courtesy of *Popular Mechanics Magazine*).

main rotor torque. The method proved in theory to provide tracking controllers for a wide class of trajectories, including aggressive trajectories involving extreme attitude angles. However, the mathematical model used for design and evaluation of this controller relied on a number of unrealistic assumptions, including exact knowledge of the tail rotor torque and moments of inertia and instantaneous application of precisely known control moments.

The key enabling step toward the development of the necessary control logic to execute extreme maneuvers was the study and mathematical modeling of pilot's control modality. We analyzed the human pilot's strategies from time histories of its commands and the vehicle state variables that were recorded from different piloted maneuvers.¹⁵ The results build on a series of efforts that started with the development of an avionics package for an acrobatic miniature helicopter,¹⁶ followed by the development and validation of a nonlinear dynamic model valid across a broad range of flight conditions^{17,18} and the design of trim flight control, which were used to provide reliable initial conditions for the maneuver entry and safe recovery at maneuver exit. At the same time, these controllers are used to operate the helicopter in nominal flight conditions.

The ability to execute maneuvers automatically is beneficial for autonomous flight. For example, the maneuvering capability can be used for a reactive obstacle or threat avoidance system. It can also be used by a higher-level motion planning algorithm, giving access to a broad range of vehicle behaviors when the trajectory optimization is performed. For example, Frazzoli et al.¹⁹ developed a path planning method that makes use of the particular structure of a so-called maneuver automaton (MA). An MA combines a finite number of fixed trim trajectories with finite duration maneuvers; the latter are used to transition among the set of trim trajectories. The hybrid control architecture presented in this paper, which results from the combination of trim flight controllers with a maneuver execution logic, motivates a more general, yet simple, hybrid representation of the vehicle behavior. Such a hybrid model, thanks to its simplicity, can help perform real-time flight-path optimization.

This paper describes the development, implementation and experimental validation of the maneuvering logic that was first outlined in Ref. 15. The flight-tests were performed on the Massachusetts Institute of Technology's (MIT's) custom instrumented autonomous helicopter. This test bed is based on a 5-ft (1.52-m) rotor X-Cell .90 helicopter, which is popular among R/C acrobatic pilots.²⁰ Several acrobatic maneuvers, including snap roll, split-S, and hammerhead were successfully performed.²¹ After a brief description of the helicopter, avionics, and trim flight-control system, we describe the key results from the analysis of the human pilot strategy. Subsequently, we describe the development of the human-inspired maneuvering

control logic¹⁵ used for the implementation of acrobatic maneuvers. Then we present flight-test validation data that were collected during a variety of automatically executed maneuvers, as well as an entire sequences of maneuvers. Finally, we present a hybrid model based on a simplified description of the closed-loop behavior, combining the trim tracking and maneuvering capabilities that are enabled through our system.

Maneuvering Flight Experiments and Analysis

Experimental Platform

An X-Cell .60 hobby helicopter²⁰ from Miniature Aircraft USA was used to flight test the automatic aerobatics algorithms. The helicopter weighs close to 10 lb empty and 17 lb with the custom avionics payload¹⁶; the aircraft retains good aerobatic capabilities with the payload. The hingeless main rotor is equipped with a Bell-Hiller stabilizer bar (see Refs. 4 and 22), which provides lagged attitude rate feedback and augments the servo. The helicopter is powered by a piston engine running on a mixture of methanol, nitromethane, and oil. In the course of the project, we replaced the original engine (engine capacity 0.6 in.³, or 10 cm³, with maximum horsepower of approximately 2.2) with a more powerful one (0.9 in.³ or 15 cm³, and maximum 3 hp) to increase the thrust margin and maneuvering capabilities. A full tank of fuel (1 lb) provides about 9 min flight time. The helicopter is equipped with an electronic governor, an off-the-shelf device that maintains the rotor speed constant to a set value (1600 rpm) via a proportional-integral controller. The active yaw-rate damping system that is typically realized by a yaw rate gyro and feedback system on R/C helicopters is implemented on our aircraft with our own controller and measurements from the inertial measurement unit. Note that this yaw damping controller is always enabled. Figure 2 shows the X-Cell helicopter in flight with the custom avionics box. It is mounted on a suspension system to isolate the sensors and electronics from vibrations.

Trim-Flight and Maneuvering-Flight Regimes

From observation of acrobatic flight, we can readily recognize two distinct flight regimes: following trim trajectories and performing maneuvers.^{15,23} Between the maneuvers, the pilot uses fine adjustments to maintain equilibrium trajectories, which can be characterized by forward speed, side-slip angle, climb rate, and turn rate. The dynamic behavior in this flight regime is, in general, adequately described by linear models, and can be automated by the use of control design methods developed for linear time-invariant (LTI) systems. The maneuvering portion of the flight involves much larger control inputs, and the full available range is often used. The vehicle state variables, such as angular rates, attitude, and speed, undergo large and rapid variations. An LTI model cannot adequately describe the vehicle dynamics in this flight regime. Moreover, during some segments of the maneuvering flight, the vehicle is uncontrollable



Fig. 2 Instrumented X-Cell helicopter in flight.

in the control-theoretic sense. For example, when the aircraft is banked 90 deg, it cannot maintain its altitude. These factors make it difficult, or impossible, to track aerobatic state trajectories with linear control design methods, or with approaches based on feedback linearization.

Figure 3 shows the behavior of the aircraft through the combination of trim flight and maneuvering flight.

Trim Flight Controllers

Experiments involving aerobatic flight require safe recovery from a broad range of flight conditions. Recovery by an expert R/C pilot is not trivial because the pilot is not actively controlling the helicopter during the automated portion of the flight. Therefore, much time was invested in the design and testing of the trim flight controllers.

Among different linear control design methodologies, the linear quadratic regulator (LQR) provides for good robustness to plant uncertainties for systems with full-state feedback.²⁴ Modeling based on a combination of first principles and identification techniques was used to develop a nonlinear model. The model was successfully validated up to an airspeed of 20 m/s (Refs. 17 and 18).

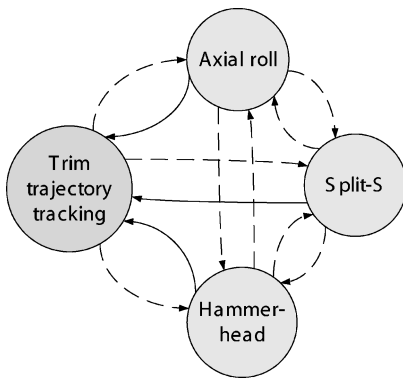


Fig. 3 State-machine representation of helicopter behavior combining trim and maneuvering flight: ---, transitions allowed based on vehicle state.

The longitudinal-vertical and lateral-directional dynamics of the X-Cell are sufficiently decoupled in low advance-ratio flight (up to $\mu = 0.15$, which corresponds to about 20 m/s) to design separate feedback controllers for the two subsystems. The dynamics of helicopter change significantly between hover and cruise flight. This was addressed by gain scheduling the LQR controller with forward speed, which enabled good tracking performance across the range of speeds required for aerobatic flight. Flight-test evaluations also showed reliable recovery from a range of initial conditions.

Analysis of the Human Pilot's Maneuvering Strategy

In this paper we present an approach to the automatic execution of maneuvers that is inspired by the human pilot's strategies.¹⁵ Based on the input and state time histories recorded during a series of piloted aerobatic maneuvers, we made the following observations: each particular type of maneuver exhibits largely repeatable characteristics; the pilot uses little continuous feedback type actions; most of the pilot's actions can be parameterized by piecewise constant, or piecewise linear, functions, with the switching times determined by the vehicle attitude. To illustrate this, consider the superposed state and control time histories, from a series of longitudinal axial roll maneuvers, shown in Fig. 4.

During the roll maneuver, the pilot primarily uses the lateral cyclic and collective pitch control inputs. Proportional yaw rate feedback to the tail rotor pitch is always active during the maneuver and helps stabilize the helicopter about the vertical axis. From the collected time histories, we can see that the commands follow a simple scheme: They are either held constant or changed as linear functions of time. The duration of the ramp-up and ramp-down of the commands varies between 0.2 and 0.4 s. These pilot inputs are performed in a feedforward fashion; the timescale is too small to allow continuous feedback by the pilot. The pilot also refrains from the use of abrupt steplike commands, which would excite the lightly damped couple rotor-stabilizer-fuselage mode.²⁵ We believe that the pilot actually performs some rudimentary input shaping to achieve a smooth angular response. Both the magnitude and the duration of the ramp across different instances of the same maneuver are highly repeatable. Therefore, it is reasonable to assume that segments of

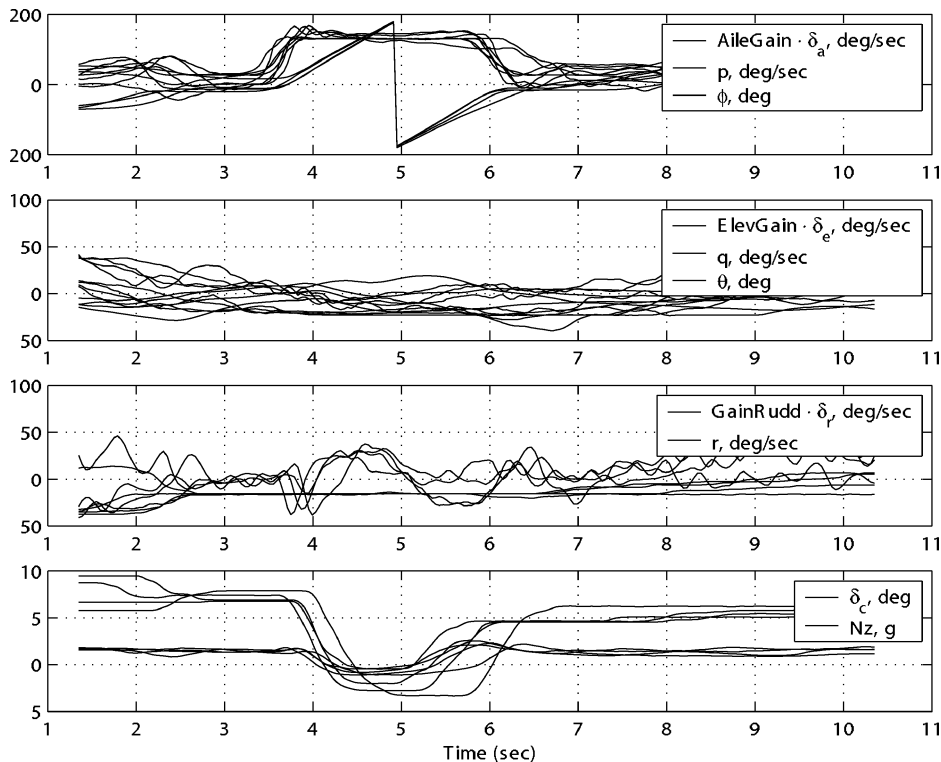


Fig. 4 Recorded state and input time histories for multiple axial roll maneuvers; variables of interest are pilot lateral cyclic control δ_a , helicopter roll angle ϕ , and pilot collective control δ_c .

the input sequence used for the implementation of the maneuver have been learned by the pilot.

Given the simple parameterization of the pilot commands, a key question is the timing of the different segments of the input sequence. We need to determine what triggers the command transitions between the different segments of the piecewise linear control input profiles. At the start of the maneuver, the pilot ramps a particular command to the desired magnitude, for example, maximum lateral cyclic at the start of an axial roll. By analysis of the timing of the start of the ramp down of the lateral cyclic command, we observed that it correlates with the bank angle, that is, for the roll maneuver, the ramp down starts when the helicopter is short of being level by about 50 deg. This type of triggering matches with the instructions given in fixed-wing aerobatics handbooks.²⁶ An analysis of the use of the cyclic and tail rotor commands in other maneuvers (split-S, hammerhead, loop) shows the same principle: An attitude-based trigger signal is used to switch the commands between different portions of piecewise linear sequence.

In Fig. 4 we can see that the collective control input, although also seemingly piecewise linear, is less repeatable than the cyclic commands across different instances of the same maneuver. The timing of the collective command, that is, rotor trust, is critical for maintenance of altitude and minimization of course changes during the maneuver. Conceivably, by trial and error, the pilot would learn a pattern that results in a properly executed maneuver. A good candidate for collective input modulation law during maneuvers can be inferred from first principles. For example, during an axial roll, the main objectives would be to achieve a close-to-constant vertical lift component, constant propulsive thrust, and little lateral forces throughout the maneuver. Note that these objectives are not physically feasible. However, they can be approximated. A modulation law that is based on a cosine function of bank angle would provide a trim thrust during level attitude flight ($\phi = 0$ -deg roll angle), negative trim thrust during inverted flight ($\phi = 180$ deg), and zero thrust when the rotor disc is perpendicular to the horizon ($\phi = 90$ and 270 deg). This basic modulation law seems applicable to other maneuvers as well.

Control Augmentation for the Maneuvering Flight

Despite the apparent simplicity of the human pilot's strategies for maneuver execution, implementing them in a completely open-loop fashion will not provide repeatable trajectories. The helicopter is an unstable dynamic system, highly sensitive to atmospheric disturbances. An entirely open-loop implementation of the control input segments will inevitably result in important variations in trajectories between runs. The pilot may be making some fine adjustments, based on the aircraft state, that are not captured by our proposed command framework, for example, in the length of the ramp intervals and levels of commands.

We decided to augment the bare airframe with roll, pitch, and yaw rate tracking controllers. This reduces the uncertainty in the aircraft's angular responses, which are key variables in the maneuver execution. The rate tracking loops are single-axis proportional–integral controllers. Notch filters are applied on the cyclic commands. These prevent an excitation of the lightly damped rotor–stabilizer–fuselage modes²⁵ and allow a higher controller bandwidth.

From piloted flight testing with these angular rate tracking controllers, we have found that the pilot's strategy remains largely unchanged. With this setup, the pilot commands the roll, pitch, and yaw rates, together with the collective pitch angle. Figure 5 shows the state and control time histories for an axial roll performed with the rate command system. Figure 6 shows the approximation of the pilot's rate commands with piecewise linear functions. As can be seen, the ramp-up and ramp-down times are on the order of 0.2–0.4 s. As is typical for the axial roll maneuver, the ramp-down starts when the bank angle reaches -50 deg (for a roll to the right). Finally, we can see the closed-loop roll rate response is similar to the open-loop response: It has a fast rise time (≈ 0.2 s) and a second-order characteristic, although it is better damped.

For other maneuvers, the same approach was used. The pilot performed several types of maneuvers with these angular rate tracking

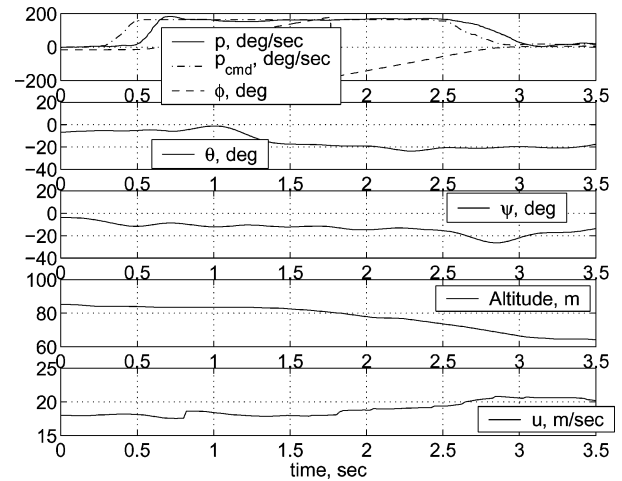


Fig. 5 Recorded state trajectory during axial roll with rate tracking controllers.

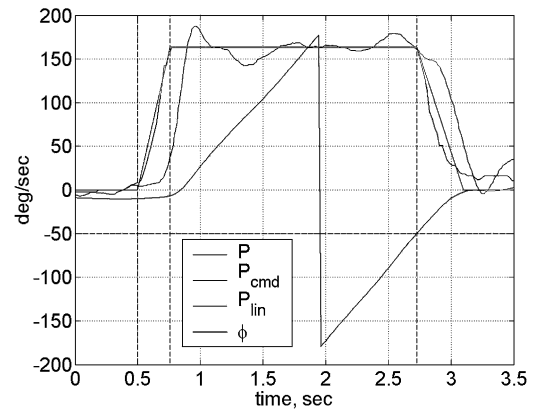


Fig. 6 Comparison between the pilot roll rate command and its piecewise linear approximation.

controllers. The resulting angular rate trajectories for each maneuver type were then approximated with the piecewise linear parameterization. The specific attitudes used in the triggering of the rate commands were inferred from the recorded pilot rate commands and aircraft attitude time histories. These approximations of the rate trajectories serve as the reference commands for the angular rate tracking loops during the automatic execution of the maneuvers. The resulting rate command trajectories were then implemented in software as simple state machines, which will be described next.

Human-Inspired Logic for Automatic Maneuvering

The sequence for an automatic maneuver execution requires switching from the trim flight controllers to the maneuver control logic and back. In both cases, the controllers have as many integrator states as control surfaces; therefore, it is possible to initialize the integrator states such that the surface deflections remain continuous. This logic enables smooth transitions between the modes.

Maneuver entrance and exit are two critical phases for implementation. To ensure a minimum variation in the maneuver entry conditions, we introduced a leveling phase, which uses decoupled proportional attitude controllers with inner-loop rate feedback to level the helicopter (within 3 deg in roll and pitch). During this phase, the yaw rate feedback is maintained, and the collective pitch angle is kept constant. Thanks to our attitude control loops, this phase is short (less than one-half of a second); for additional safety, a timeout is used as well. To guarantee stable recovery from the maneuvers, the helicopter has to settle for a length of time in the trim flight-control mode before it can proceed with the execution of another maneuver. The settling duration was set to 2 s based on simulations and actual flight experiments.

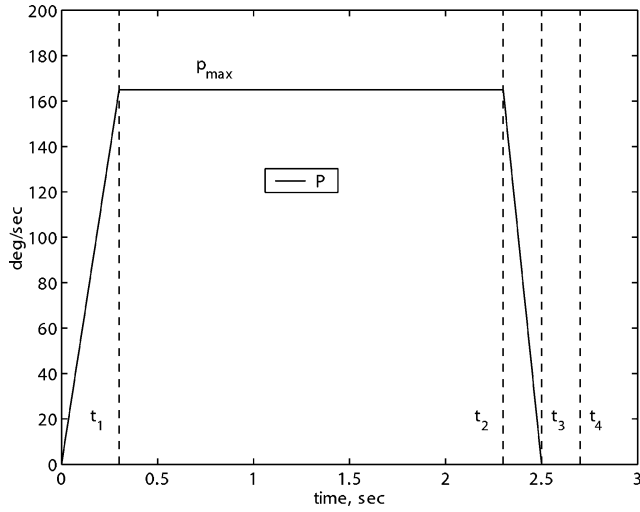


Fig. 7 Reference roll rate trajectory for axial roll maneuver.

Essentially, the implementation of any maneuver includes the following three phases: 1) leveling, 2) following the piecewise linear angular rate trajectories and collective pitch profile corresponding to the specific maneuver, and 3) settling. The leveling and settling conditions were realized by the use of an execution logic. The logic also checks if the helicopter meets speed and altitude requirements. If the exit conditions are satisfied at each phase, the maneuver execution is carried out; if, on the other hand conditions are not met, the execution is automatically aborted. This schedule allows the safe sequence of a series of maneuvers. This capability was demonstrated by execution of a preprogrammed airshow routine fully automatically.

Axial Roll Maneuver

The reference trajectories for the angular rates were generated by the use of the piecewise linear parameterization. The pitch and yaw rate commands were set to zero throughout the maneuver. The roll rate profile, shown in Fig. 7, was modeled as follows: 0.3-s linear ramp up to $p_{\max} = 165$ deg/s (t_1); constant command until the helicopter bank angle reaches 310 deg (t_2); 0.2-s linear ramp-down to zero commanded roll rate (t_3); 0.2-s coasting time at zero roll rate command to allow leveling after the maneuver (t_4).

We decided not to use the Euler attitude angles during aerobatic maneuvers because of their known singularities when the helicopter reaches +90- or -90-deg pitch angle. Instead, we used an approximate roll angle obtained by integration of the body axis roll rate after the maneuver initiation. This approximate roll angle was used to determine the initiation time of the ramp-down start (t_2). Alternatively, one could also utilize a measure of distance between the current and the target attitudes as used by Bullo²⁷ and Frazzoli.¹⁴

The collective pitch angle was modulated as the cosine function of the angle between the local vertical and the aircraft's body Z axis:

$$\delta_{\text{col}} = \max(\delta_{\text{col}}^{\text{trim}} \cdot \cos \phi \cos \theta, \delta_{\text{col}}^{\text{min}}) \quad (1)$$

where $\delta_{\text{col}}^{\text{trim}}$ is the trim collective angle in forward cruise flight. This strategy results in a profile that is close to the pilot's actions during the roll. We limited the negative collective angle to $\delta_{\text{col}}^{\text{min}} = -3$ deg (full range is from -10.5 to 10.5 deg) to retain sufficient control authority during portions of the flight with negative rotor loading; this approach is also used by pilots.

Figure 8 shows the flight-test data for an automatic axial roll. Note that the changes of heading angle, speed, and altitude are small between the maneuver initiation and exit, which is typically desired for an axial roll maneuver.

Split-S Maneuver

Another maneuver that was analyzed and implemented by the use of the human-inspired approach is the split-S (Fig. 1). This is a more elaborate maneuver, which combines different maneuver elements.

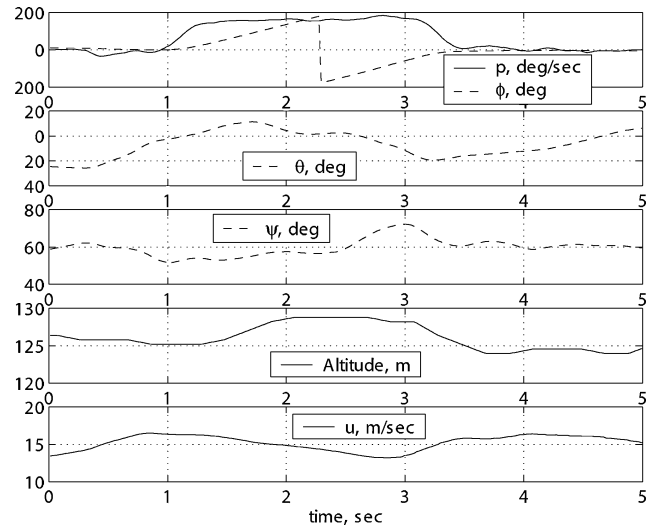


Fig. 8 Recorded state trajectory during automatic axial roll.

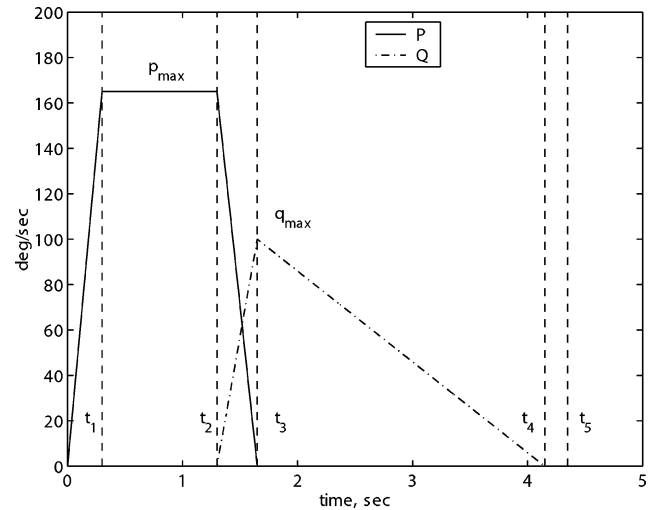


Fig. 9 Pitch and roll rate reference trajectories for split-S maneuver.

The yaw rate command is kept at zero during the entire sequence. The roll and pitch rate commands are shown in Fig. 9. Here, the start of the roll rate ramp-down t_2 and the pitch rate ramp-down t_4 are determined by achievement of the specific pseudoattitude roll and pitch angles ϕ_d and θ_d :

$$t_2 : \int_0^{t_2} p \, dt = \phi_d \quad (2)$$

$$t_4 : \int_{t_3}^{t_4} q \, dt = \theta_d \quad (3)$$

The collective pitch command follows the cosine rule given in Eq. (1).

Figure 10 shows the recorded state trajectories during an automatic split-S maneuver. The helicopter dropped a total of 30 m and reached 18 m/s during the drop, which is slightly more than during a piloted execution. Both effects were predicted during simulation. The total heading change from the entry until the exit of the maneuver was within 5 deg of the desired 180 deg.

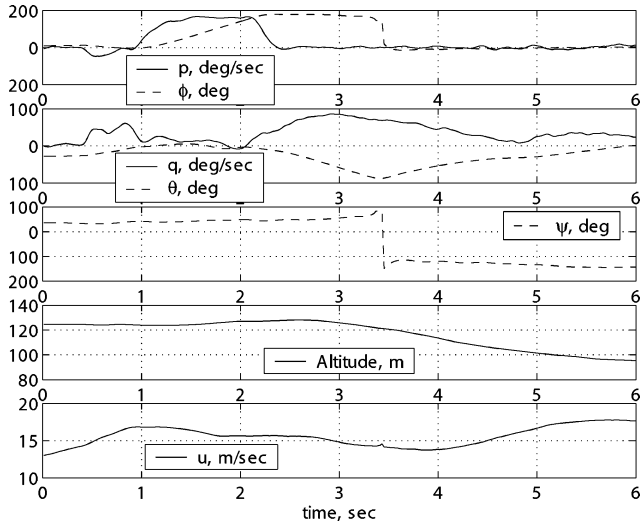
Flight-Test Demonstration

Flight-Test Procedure

To facilitate with the flight testing of the control laws, the trim flight controllers were set up in several control modes (Table 1). A

Table 1 Autopilot modes for MIT X-Cell Helicopter

Axis	Manual	Rate tracking	VHRC AH	Hover hold
Longitudinal	Longitudinal Cyclic	Pitch rate	Forward velocity	Position
Lateral	Lateral Cyclic	Roll rate	Side velocity	Position
Directional	Yaw rate	Yaw rate	Turn rate	Heading
Vertical	Collective	Collective	Altitude/rate	Altitude

**Fig. 10** Recorded state trajectory during automatic split-S.

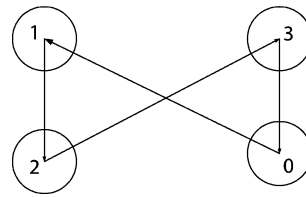
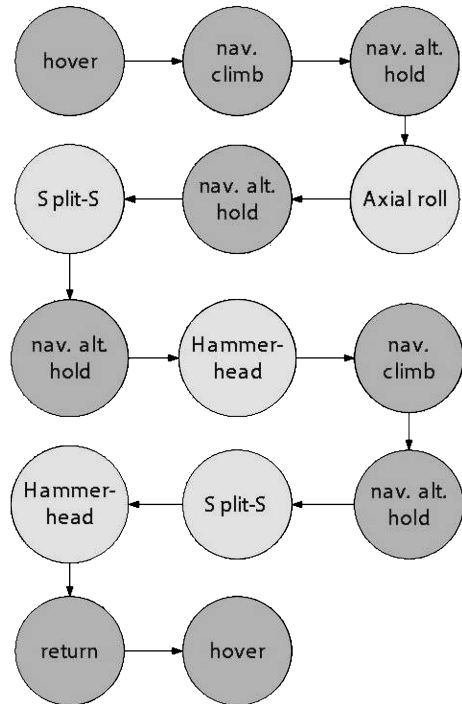
regular two-stick R/C transmitter unit is used to uplink pilot commands to the flight-control computer. In the manual mode, the pilot commands the main rotor collective and cyclic pitch deflections on the transmitter sticks, as well as a setpoint for a yaw rate feedback controller. In the rate tracking mode, the pilot commands all three angular rates and the collective pitch. In the velocity/heading rate command–altitude hold (VHRC AH) mode the pilot commands turn rate, forward, side, and vertical velocities. (The operator has an option to engage altitude hold.) In the hover hold mode, the helicopter maintains global positioning system (GPS) position, pressure altitude, and heading.

The pilot can initiate a preprogrammed sequence by activating a switch on the R/C transmitter. The sequence can include either a single aerobatic maneuver or an aerobatic routine, where the helicopter follows selected GPS waypoints, performs aerobatic maneuvers at specified locations, and returns to hovering flight at the starting point.

The first flight test of each of the automatic maneuvers proceeds as follows: 1) The pilot takes off manually, and engages the VHRC AH mode at a safe maneuver altitude. 2) The pilot commands the forward speed setpoint used for the maneuver execution (12 and 15 m/s were used). From that point, the helicopter is flown with a single left sideways stick–turn rate (or, equivalently, bank angle) command. The autopilot maintains the altitude and forward speed setpoints. 3) After performing a number of turns to attain the desired course and position, the pilot brings the helicopter to level flight by commanding zero turn rate (releasing the spring-loaded stick). 4) The pilot then engages an entirely automatic maneuver sequence by a switch on the R/C transmitter. The helicopter performs the maneuver and exits the sequence at a close to level altitude and practically zero angular rate. 5) At this point, the controller automatically goes back to the VHRC AH mode. The altitude hold acquires a new setpoint, and the forward speed returns to the selected speed setting.

Autonomous Airshow

To demonstrate transitions between trim trajectory modes and automatic maneuvering, as well as the sequencing of several maneuvers, we implemented an autonomous airshow routine. The basic idea of that routine was for the helicopter to follow a figure-8 pattern

**Fig. 11** Figure 8 waypoint route for autonomous airshow routine.**Fig. 12** State-machine representation for automatic execution of airshow routine.

defined by four waypoints (shown in Fig. 11) and perform single or sequenced maneuvers on specified laps. The entire routine was preprogrammed; no human intervention was used at any time during the sequence. A conventional guidance algorithm based on the minimization of the cross-track error was used for waypoint tracking. The routine was implemented as a state machine as illustrated by the graph in Fig. 12.

Once the routine is engaged, the helicopter proceeds with a vertical climb to 50-m altitude above ground level (AGL), at which time it transitions into waypoint navigation flight and continues to climb to the final 120-m AGL level, where the helicopter continues waypoint navigation while holding the altitude. The first maneuver is initiated 100 m before reaching waypoint 1. On the exit from the axial roll, the helicopter heads toward waypoint two holding the exit altitude, and continues waypoint navigation. When it is back on the leg from waypoint 0 to waypoint 1, at the same 100-m distance from waypoint 1, the split-S is initiated. On exit from split-S, the helicopter heads toward waypoint 3, then 0, where it performs a hammerhead maneuver where previous maneuvers were executed. After the hammerhead, the helicopter continues waypoint navigation starting with waypoint 3, while climbing back to 120-m AGL. On reaching the target altitude, the helicopter continues waypoint navigation in altitude hold until it is back in the maneuvering region and initiates a split-S followed immediately by a hammerhead. At this point, the helicopter flies back to departure point and transitions to hover, waiting for further commands.

Figure 13 shows flight data from the split-S–hammerhead sequence. Note that the minimum entry speed for the hammerhead maneuver was defined as 14 m/s; at the exit of the split-S maneuver, the helicopter had sufficient speed to perform it.

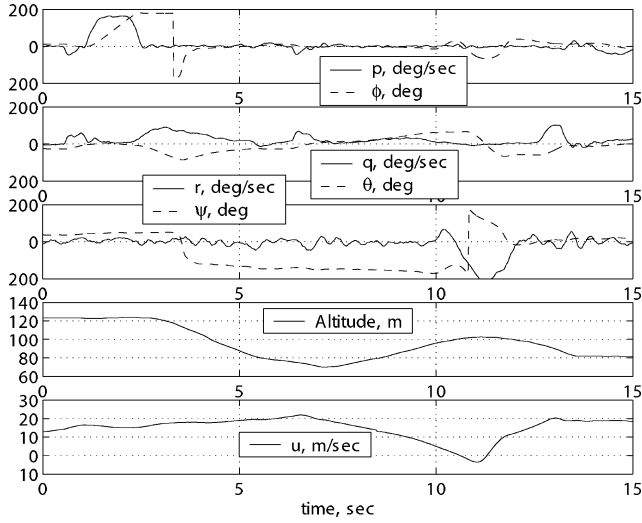


Fig. 13 Flight data for automatic split-S-hammerhead sequence.

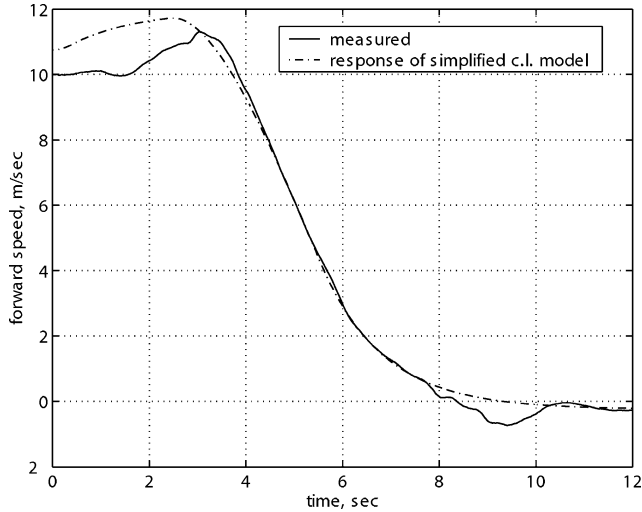


Fig. 14 First-order approximation of closed-loop velocity response.

Hybrid Closed-Loop Model

The combination of trim flight controllers and maneuvering results in dynamic capabilities that are broader than that which is achieved with conventional feedback control systems. For autonomous flight, path-planning algorithms that can explicitly account for the full range of vehicle maneuvering capabilities are desirable. In the following, we describe a mathematical representation of the vehicle dynamics under our hybrid control architecture that can be used for motion planning.

Under our hybrid control architecture, at any point in time, the aircraft is either following a trim trajectory (by the use of the trim tracking controllers) or maneuvering (by the use of the maneuvering logic). The resulting vehicle behavior can be conveniently represented by the use of a hybrid state-machine model. Figure 3 shows the graph for such a state machine with three maneuvers and the trim flight controller. For example, this low-order representation may be used by guidance algorithms involving real-time optimization.²⁸

The aircraft behavior under the trim flight controller can be effectively described by the resulting closed-loop equations of motion. These equations can often be simplified by low-order transfer functions. By design, the closed-loop response to forward velocity, vertical velocity, and turn rate commands exhibit characteristics of second-order systems with small overshoot (5–10%). Furthermore, the amount of cross coupling in the closed-loop response should be small; a first-order approximation of the primary closed-loop responses is often sufficient. Figure 14 shows the comparison of the

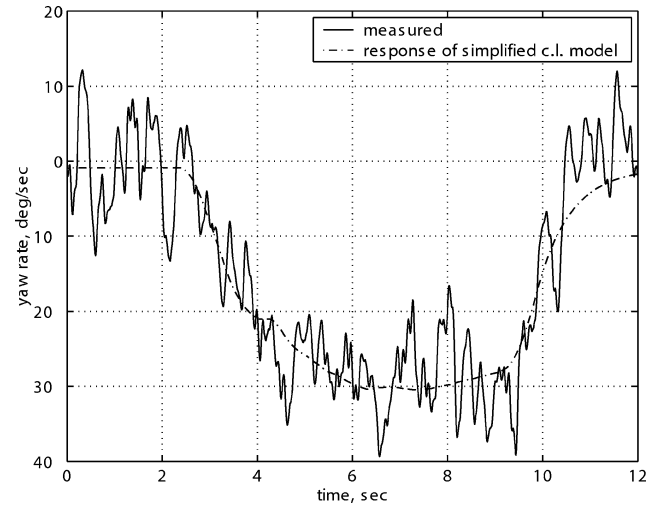


Fig. 15 First-order approximation of closed-loop yaw rate response.

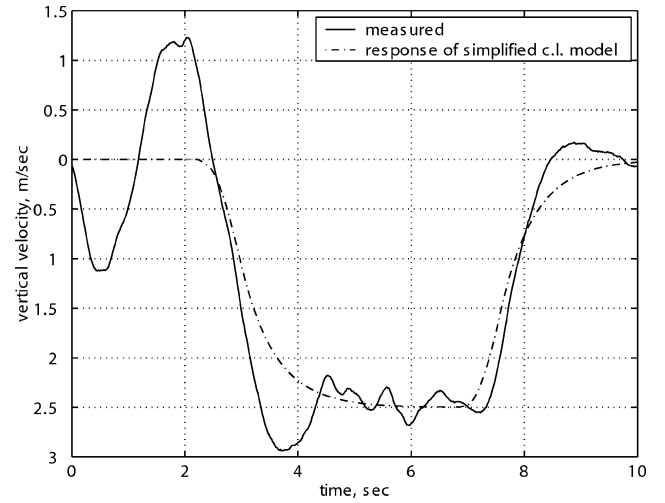


Fig. 16 First-order approximation of closed-loop altitude rate response.

actual longitudinal closed-loop velocity response and its first-order approximation. Figure 15 shows the comparison for the yaw rate (which is close to turn rate). The yaw rate signal is noisy for a number of reasons (residual vibration, engine rattle producing torque transients, and coarse quantization of the tail rotor actuator, which leads to a limit-cycle pattern). Nevertheless, one can see that the low-frequency trend is captured well by the first-order approximation. Finally, Figure 16 shows the comparison for the altitude rate. The poor match in the beginning of the segment is due to cross coupling with the lateral-directional response: The helicopter performed a banking turn. This shows that the approximate model is far from ideal; however, it represents a reasonably realistic representation of the dynamics with a very low number of states.

By the use of the aforementioned approximations for the closed-loop dynamics, we can write the following simplified model, which includes heading and three-dimensional inertial positions:

$$\dot{u} = -(1/\tau_u)u + (1/\tau_u)u_c, \quad \tau_u = 1.3 \text{ s}$$

$$\dot{r} = -(1/\tau_r)r + (1/\tau_r)r_c, \quad \tau_r = 0.7 \text{ s}$$

$$\dot{V}^h = -(1/\tau_h)V^h + (1/\tau_h)V_c^h, \quad \tau_h = 0.6 \text{ s}$$

$$\dot{\psi} = r, \quad \dot{p}_N = u \cos \psi \quad \dot{p}_E = u \sin \psi \quad \dot{h} = V^h$$

Note that, whereas the open-loop dynamics change significantly from hover to forward flight, the time constants of the closed-loop responses are close to being constant.

The aircraft behavior under the maneuvering logic, for the purpose of motion planning, can be represented as a discrete state update. For a specific maneuver k , we have

$$\psi(t + \Delta T_k) = \psi(t) + \Delta\psi_k + w_{\psi,k} \quad (4)$$

$$p_N(t + \Delta T_k) = p_N(t) + \Delta p_{N,k} + w_{p_N,k} \quad (5)$$

$$p_E(t + \Delta T_k) = p_E(t) + \Delta p_{E,k} + w_{p_E,k} \quad (6)$$

$$h(t + \Delta T_k) = h(t) + \Delta h_k + w_{h,k} \quad (7)$$

where ΔT_k and $\Delta_{\bullet,k}$ are, respectively, the duration and state transition resulting from maneuver k . Note that our current maneuver execution logic does not permit tight compensation for disturbances during the maneuvering phase. Therefore, the same maneuver can exhibit variations in the resulting duration and state transition. For now, we represented this uncertainty through a disturbance $w_{\bullet,k}$; Monte Carlo simulations and flight experiments can help characterize the type and extent of these variations.

Conclusions

The human-inspired approach used for the development of maneuvering logic has so far been the only demonstrated approach to the control of a small-scale helicopter across the highly nonlinear aerobatic flight regime. With the hybrid control architecture that combines the maneuvering logic and the trim trajectory controllers, we have been able to demonstrate flight capabilities similar to that of expert human pilots.

Such a hybrid architecture permits taking advantage of a broad range of vehicle behavior, from continuous precision flight to agile maneuvering. This is a fundamental capability for autonomous flight with agile vehicles. Moreover, under such a control architecture, the vehicle behavior can be described in a more economical fashion using a low-order hybrid representation. Such a hybrid model lends itself well for path planning based on real-time optimization.

We also realize that more work is required in several areas to take full advantage of this approach. In particular, it is necessary to "robustify" the maneuver's implementation to make their execution more repeatable in the presence of disturbances and modeling uncertainties. It would also be highly beneficial if a maneuver could be parameterized to allow flexibility in the resulting state variation. For example, the split-S could be used to achieve a range of heading changes beyond the nominal 180 direction reversal.

Acknowledgments

Partial funding for this research was provided by the U.S. Office of Naval Research (ONR) under a Young Investigator Award and ONR Grant N000140310171, NASA Grants NAG2-1441 and NAG2-1522, DARPA Grant F33615-01-C-1850, and AIAA Foundation Graduate Award in Guidance, Navigation, and Control. Essential participants in this effort include the Massachusetts Institute of Technology graduate students Ioannis Martinos, Kara Sprague, Rodin Lyasoff, and Alex Shterenberg. We would like to thank David Vos of Athena Technologies, who provided invaluable advice throughout all phases of the project, and M. Piedmonte, now with Athena Technologies, and formerly at Draper Laboratory, for supporting early experiments with the X-Cell .60 helicopter.

References

- ¹"Unmanned Aerial Vehicles Roadmap 2002-2007," Memo, Dept. of Defense, Dec. 2002.
- ²Murphy, J., Walker, H., and Kaufman, A., "An Integrated Low Altitude Flight Control System for Helicopters," AGARD CP 86, AGARD, June 1971.
- ³Mettler, B., *Identification, Modeling and Characteristics of Miniature Rotocraft*, Kluwer Academic, Boston, MA, 2002, Chap. 5.
- ⁴Miller, R. H., "A Method for Improving the Inherent Stability and Control Characteristics of Helicopters," *Journal of Aeronautical Sciences*, Vol. 17, No. 6, 1950, pp. 363-376.
- ⁵Padfield, G. D., *Helicopter Flight Dynamics: The Theory and Application of Flying Qualities and Simulation Modeling*, AIAA Education Series, AIAA, Reston, VA, 1996, p. 17.
- ⁶Tischler, M. B., Colbourne, J. D., Morel, M. R., Biezad, D. J., Cheung, K. K., Levine, W. S., and Moldoveanu, V., "A Multidisciplinary Flight Control Development Environment and its Application to a Helicopter," *IEEE Control Systems Magazine*, Vol. 19, No. 4, 1999, pp. 22-33.
- ⁷Tischler, M. (ed.), *Advances in Aircraft Flight Control*, Taylor and Francis, Cornwall, England, U.K. 1996, pp. 3-33.
- ⁸Yavrucuk, I., Prasad, J. V. R., and Calise, A. J., "Adaptive Limit Detection and Avoidance for Carefree Maneuvering," AIAA Paper 2001-4003, Aug. 2001.
- ⁹Osder, S., and Caldwell, D., "Design and Robustness Issues for Highly Augmented Helicopter Controls," *Journal of Guidance, Control, and Dynamics*, Vol. 15, No. 6, 1992, pp. 1375-1380.
- ¹⁰LaCivita, M., Kanada, T., Papageorgiou, G., and Messner, W., "Design and Flight Testing of a High-Bandwidth h-Infinity Loop Shaping Controller for a Robotic Helicopter," AIAA Paper 2002-4836, Aug. 2002.
- ¹¹Kannan, S., and Johnson, E., "Adaptive Trajectory Based Control for Autonomous Helicopters," AIAA Paper 2002-358, Oct. 2002.
- ¹²Bryson, A., *Control of Aircraft and Spacecraft*, Princeton Univ. Press, Princeton, NJ, 1994, pp. 179-181.
- ¹³McRuer, D., Ashkenas, I., and Graham, D., *Aircraft Dynamic and Automatic Control*, Princeton Univ. Press, Princeton, NJ, 1974, Chap. 1.
- ¹⁴Frazzoli, E., "Robust Hybrid Control for Autonomous Vehicle Motion Planning," Ph.D. Dissertation, Dept. of Aeronautics and Astronautics, Massachusetts Inst. of Technology, Cambridge, MA, 2001.
- ¹⁵Gavrilets, V., Frazzoli, E., Mettler, B., Piedmonte, M., and Feron, E., "Aggressive Maneuvering of Small Autonomous Helicopters: A Human-Centered Approach," *International Journal of Robotics Research*, Vol. 20, No. 10, 2001, pp. 795-807.
- ¹⁶Sprague, K., Gavrilets, V., Duglaj, D., Mettler, B., and Feron, E., "Design and Applications of an Avionics System for a Miniature Acrobatic Helicopter," *AIAA Digital Avionics System Conference Proceedings*, AIAA, Reston, VA, 2001, pp. 3.C.5-1-3.C.5-10.
- ¹⁷Gavrilets, V., Mettler, B., and Feron, E., "Nonlinear Model for a Small-Size Acrobatic Helicopter," AIAA Paper 2001-4333, Aug. 2001.
- ¹⁸Gavrilets, V., Mettler, B., and Feron, E., "Dynamic Model for X-Cell 60 Helicopter in Low Advance Ratio Flight," Tech. Rept. P-2543, Lab. for Information and Decision Systems, Massachusetts Inst. of Technology, Cambridge, MA, Dec. 2002.
- ¹⁹Frazzoli, E., Dahleh, M., and Feron, E., "Real-Time Motion Planning for Agile Autonomous Vehicles," *Journal of Guidance, Control, and Dynamics*, Vol. 25, No. 1, 2002, pp. 116-129.
- ²⁰"X-Cell .60 Graphite SE Helicopter Kit (Special Edition) Instruction Manual," Miniature Aircraft USA, Orlando, FL, 1999.
- ²¹Gavrilets, V., Martinos, M., Mettler, B., and Feron, E., "Control Logic for Automated Aerobatic Flight of Miniature Helicopter," AIAA Paper 2002-4834, Aug. 2002.
- ²²Bramwell, A. R. S., *Bramwell's Helicopter Dynamics*, AIAA, Reston, VA, 2001, pp. 176-178.
- ²³Piedmonte, M., and Feron, E., "Aggressive Maneuvering of Autonomous Aerial Vehicles: A Human-Centered Approach," *International Symposium on Robotics Research*, Oct. 1999.
- ²⁴Anderson, B., and Moore, J., *Optimal Control: Linear Quadratic Methods*, Prentice-Hall, New York, 1990.
- ²⁵Mettler, B., Tischler, M. B., and Kanade, T., "System Identification Modeling of a Small-Scale Unmanned Rotorcraft for Control Design," *Journal of the American Helicopter Society*, Vol. 47, No. 1, 2002, pp. 50-63.
- ²⁶Deakin, R., *Model Helicopter Aerobatics*, Traplet Publications, Worcestershire, England, U.K., 2000.
- ²⁷Bullo, F., "Nonlinear Control of Mechanical Systems: A Riemannian Geometry Approach," Ph.D. Dissertation, Dept. of Control and Dynamical Systems, California Inst. of Technology, Pasadena, CA, Aug. 1998.
- ²⁸Schouwenaars, T., Mettler, B., Feron, E., and How, J., "Hybrid Architecture of Full-Envelope Autonomous Guidance," 59th Forum of the American Helicopter Society, May 2003.